Available online at www.sciencedirect.com
SCIENCE DIRECT®
Journal of Sound and Vibration 287 (2005) 571–589
JOURNAL OF SOUND AND VIBRATION
www.elsevier.com/locate/jsvi

The dynamic stiffness matrix of two-dimensional elements: application to Kirchhoff's plate continuous elements

J.B. Casimir[a,*], S. Kevorkian[b], T. Vinh[a]

[a]*LISMMA, Institut Supérieur de Mécanique de Paris, 3, rue Fernand Hainaut, 93407 Saint-Ouen Cedex, France*
[b]*Socotec Industrie, 1, avenue du parc, 78180 Montigny-le-Bretonneux, France*

Received 12 June 2003; received in revised form 15 November 2004; accepted 18 November 2004
Available online 10 February 2005

Abstract

This paper describes a procedure for building the dynamic stiffness matrix of two-dimensional elements with free edge boundary conditions. The dynamic stiffness matrix is the basis of the continuous element method. Then, the formulation is used to build a Kirchhoff rectangular plate element. Gorman's method of boundary condition decomposition and Levy's series are used to obtain the strong solution of the elementary problem. A symbolic computation software partially performs the construction of the dynamic stiffness matrix from this solution. The performances of the element are evaluated from comparisons with harmonic responses of plates obtained by the finite element method.

1. Introduction

The continuous element method [1,2] is based on the dynamic stiffness matrices of structural elements. This method is an attractive alternative to the finite element method for analysis of harmonic response of complex structures that are made up of simple structural elements. This method, often known as the "dynamic stiffness method", is related to a minimal discretization of the domain. The formulation is able to cover the entire frequency range of validity with respect to a given elastodynamic theory. Continuous elements are mainly used to describe the dynamic

*Corresponding author. Fax: +33 1 4945 2969.
E-mail address: jean-baptiste.casimir@supmeca.fr (J.B. Casimir).

0022-460X/$ - see front matter © 2004 Elsevier Ltd. All rights reserved.
doi:10.1016/j.jsv.2004.11.013

behavior of assemblies composed of straight or curved beams [3,4]. For such structures, the meshing of the domain is given by its topology. Beam elements are not discretized. Modal analysis is achieved by the use of specific algorithms [5]. The formulation is based on the strong solution of the dynamic problem formulated in the frequency domain. Fast Fourier transform algorithms could be used to obtain this solution, and this method is also known as the spectral element method [6,7]. Inverse Fourier transform is used to obtain solution in the time domain.

The strong solution allows one to describe an infinity of eigensolutions. The main idea is to build, for each element, the dynamic stiffness matrix, which is a function of the circular frequency ω of the harmonic regime. These matrices are denoted $\mathbf{K}_e(\omega)$ and describe exact relations between external forces and displacements at the tips of the element according to

$$\mathbf{K}_e(\omega).\mathbf{U}_e = \mathbf{F}_e. \tag{1}$$

Computer codes based on continuous elements have been elaborated in France [8], the UK [9,10] and Germany [11] but for their expansion, such codes need a larger library of elements, above all involving plates [12] and shells [13]. With this formulation, the mode shapes inside he element can have a great number of nodal points. In principle, this method can provide a solution for frequency responses in any bandwidth of frequencies for which the validity of the continuum elastodynamic has been fully defined. Continuous plate elements are directly deduced from the theory of vibrations of plates having simple geometries such as triangles or rectangles. This chapter in elastodynamics has been largely studied during the last 50 years since Mindlin's famous equations [14]. There is an abundant literature on this subject and it exceeds the scope of this paper to cover all the publications in this domain. Leissa [15] in his book has gathered all possible approximate solutions for vibrations for various plate geometries and for various boundary conditions. The Rayleigh–Ritz method is frequently used for calculating plate vibrations. Unfortunately, the displacement field is often too simple and thus solutions are valid only over a restricted frequency domain. The main difficulty surrounding plate's vibration problems lies in the fact that for some sets of boundary conditions (for example free edges), it is not possible to find exact solutions that satisfy all the boundary conditions. Gorman [16] suggested a solution for plates with all edges free which merits attention. The problem consists of not seeking an exact solution, which is theoretically impossible, but rather finding an approximate solution that satisfies the degree of accuracy chosen previously. Solutions are presented as infinite series which are able to describe an infinity of modes. But, in practice, the series have to be truncated. Gorman's clever method will be used in this paper. Kulla [1] in Germany was the first to present applicable solutions in plate continuous elements. Hagedorn [17] used Gorman's method to evaluate the impedance between two points inside a plate.

The main object of this paper is to present the principle of development of two-dimensional elements such as plates and how symbolic computation software could be used in this purpose. The method for construction of dynamic stiffness matrices is applied to the Kirchhoff bending elements, whereafter the method's performance is compared to that of the finite element method.

2. Two-dimensional continuous element

2.1. Elementary formulation

The continuous element formulation is based on the strong solution of the elastodynamic problem for a free boundary condition set applied on the element. For a given plate theory and under a harmonic regime of circular frequency ω, the strong formulation of the dynamic problem is given by a partial derivative system of Eq. (2) satisfied by the displacement components defined on the domain of the plate Ω. The number p of the components of the displacement vector $\mathbf{u}$ depends on the underlying elastodynamic theory. The strong formulation is also given by a set of boundary conditions (3) defined on the limit of the domain of the plate $\partial\Omega$. The free boundary conditions impose the value of several internal force components on $\partial\Omega$. These components are obtained from the derivatives of the displacement components by the force–displacement relationship.

$$\mathscr{L}_\omega(\mathbf{u}) = \mathbf{q} \quad \text{on } \Omega \tag{2}$$

with $\mathscr{L}_\omega$ being a differential operator and $\mathbf{q}$ the distributed load applied on the element domain Ω.

$$f\left(\ldots, \frac{\partial^k \mathbf{u}}{\partial x^i \partial y^j}, \ldots\right) = \mathbf{F}_{\text{ext}} \quad \text{on } \partial\Omega \tag{3}$$

with $\mathbf{f}$ being the force–displacement relationship and $\mathbf{F}_{\text{ext}}$ the external forces applied on the boundary $\partial\Omega$, x and y being spatial coordinates.

2.2. General solution

In contrast to the solution of the beam problem, general solutions of two-dimensional problems described above are not expressible with a finite combination of elementary functions. The p components u_i of the displacement solution $\mathbf{u}$ of the homogeneous equation associated to Eq. (2) will be expressed here by an infinite series of functions Eq. (4).

$$u_i(x,y) = \sum_{n=1}^{\infty} C_{\text{in}} h_{\text{in}}(x,y) \quad i \in [1,\ldots,p] \tag{4}$$

with C_{in} being integration constants depending on the boundary conditions (3) and h_{in} basis functions that satisfy the homogeneous equation associated to Eq. (2).

The numerical approach involves truncated series, hence the need to choose an integer N which allows one to adequately approximate the general solution with expression (5).

$$u_i(x,y) \approx \sum_{n=1}^{N} C_{\text{in}} h_{\text{in}}(x,y). \tag{5}$$

Choosing a suitable basis of functions h_{in}, this choice is the main object of the procedure. These functions should give a good approximation of the general solution for a small value of N.

If integration constants C_{in} are assembled in only one vector $\mathbf{C}$, the matricial form of the solution may be written according to expression (6).

$$\mathbf{u}(x,y) \approx \mathbf{H}_{\omega}(x,y).\mathbf{C}. \tag{6}$$

2.3. Boundary conditions

The second difference between beam continuous elements and plate elements is the dimension of the limit of the elementary domain $\partial\Omega$. The limit is a one-dimensional space. The boundary of beam elements is formed by 2 points, and force and displacement on the boundary are vectors in $\mathbb{R}^6$. Here, force and displacement defined on the boundary are one-variable vectorial functions. Expression (1) should be a relation between the projections of these functions on a Hilbert basis.

If the limit of the domain is defined with a two-component function of the curvilinear abscissa s noted $\mathbf{B}(s)$, expression (6) allows one to obtain the restriction $\partial\mathbf{u}(s) = \mathbf{u}(\mathbf{B}(s))$ of the displacement solution to the limit of the domain $\partial\Omega$:

$$\partial\mathbf{u}(s) \approx \mathbf{H}_{\omega}(\mathbf{B}(s)).\mathbf{C} = \partial\mathbf{H}_{\omega}(s).\mathbf{C}. \tag{7}$$

From the derivatives of the displacement components, the force–displacement relationship gives the force functions along the limit of the domain $\partial\Omega$. The vector created with these functions is noted $\partial\mathbf{f}(s)$ and is given by $\partial\mathbf{f}(s) = \mathbf{f}(\mathbf{B}(s))$. The vector $\mathbf{f}(x,y)$ is a function of the derivatives of displacement functions and is expressible with the same integration constants C_{in}. One obtains, for its restriction to the boundary,

$$\partial\mathbf{f}(s) = \partial\mathbf{G}_{\omega}(s).\mathbf{C}. \tag{8}$$

Component functions of the matrix $\partial\mathbf{G}_{\omega}(s)$ are obtained from derivation of the component functions of $\mathbf{H}_{\omega}(x,y)$ according to Eq. (3). These derivatives are then expressed on $\partial\Omega$.

2.4. Dynamic stiffness matrix

Eq. (1) relating forces components and displacement components on the limit of the domain $\partial\Omega$ is obtained from the projections of the p components of $\partial\mathbf{u}(s)$ and $\partial\mathbf{f}(s)$ on a functional basis. The dynamic stiffness matrix is afterwards obtained from the linear relation between these projections. If $(e_k(s))_{k\in\mathbb{N}}$ is a Hilbert's basis defined on the limit of the domain $\partial\Omega$, the p components of $\partial\mathbf{u}(s)$ and of $\partial\mathbf{f}(s)$ are obtained from expressions (9) and (10)

$$\partial u_i(s) = \sum_{k=1}^{\infty} \langle \partial u_i, e_k \rangle e_k(s), \quad i \in [1,\ldots,p], \tag{9}$$

$$\partial f_i(s) = \sum_{k=1}^{\infty} \langle \partial f_i, e_k \rangle e_k(s), \quad i \in [1,\ldots,p]. \tag{10}$$

The projections of the function are defined from the scalar product

$$\langle f, g \rangle = \int_{\partial\Omega} f(s)g(s)\,\mathrm{d}s.$$

In order to obtain a relation similar to Eq. (1), the series Eqs. (9) and (10) are truncated to rank M, and the $p \times M$ projections relative to each series are collected into two vectors

$$\mathbf{U}_e = \{\langle \partial u_i, e_k \rangle\}_{(i,k)\in[1,\ldots,p]\times[1,\ldots,M]} \text{ and } \mathbf{F}_e = \{\langle \partial f_i, e_k \rangle\}_{(i,k)\in[1,\ldots,p]\times[1,\ldots,M]}.$$

The components of $\partial\mathbf{H}_\omega(s)$ are noted $\partial H_{ij}(s)$ and whence the components of $\mathbf{U}_e$ are obtained from expression (11)

$$U_{(i-1)M+k} = \langle \partial u_i, e_k \rangle = \langle \partial H_{ij}, e_k \rangle C_j. \tag{11}$$

Likewise, if $\partial G_{ij}(s)$ are the components of the matrix $\partial\mathbf{G}_\omega(s)$, the components of the vector $\mathbf{F}_e$ are

$$F_{(i-1)M+k} = \langle \partial f_i, e_k \rangle = \langle \partial G_{ij}, e_k \rangle C_j \tag{12}$$

and hence, in a matricial form

$$\mathbf{U}_e = \mathbf{A}(\omega).\mathbf{C} \tag{13}$$

with $A_{(i-1)M+k,j}(\omega) = \langle \partial H_{ij}, e_k \rangle$ and

$$\mathbf{F}_e = \mathbf{B}(\omega).\mathbf{C} \tag{14}$$

with $B_{(i-1)M+k,j}(\omega) = \langle \partial G_{ij}, e_k \rangle$.

For a choice of M and N such that the matrix $\mathbf{A}(\omega)$ is square and invertible, and from expressions (13) and (14), one gets an expression similar to expression (1) with

$$\mathbf{K}_e(\omega) = \mathbf{B}(\omega).\mathbf{A}(\omega)^{-1}. \tag{15}$$

2.5. Post-processing

After assembling dynamic stiffness matrices and numerically solving the obtained linear system for a given circular frequency ω, post-processing is the operation that allows one to obtain each unknown in the elementary domain Ω. For each element, this operation is performed using expression (5) and integration constants $\mathbf{C}$. The integration constants are calculated from the displacement solution $\mathbf{U}_e$ and the inverting of expression (13).

3. Kirchhoff plate continuous element

3.1. Strong formulation

This formulation is used to build a rectangular plate according to the Kirchhoff plate theory. Constitutive material is homogeneous and isotropic and the thickness of the plate is constant.

The partial derivative system of Eq. (2) is derived from the well-known Kirchhoff plate Eq. (16) satisfied by the displacement components, i.e. the transverse displacement $w(x, y, t)$ of the middle

surface and the section's rotations β_x and β_y.

$$\begin{aligned} D\nabla^4 w + \rho h \frac{\partial^2 w}{\partial t^2} &= q(x, y, t), \\ \beta_x &= \frac{\partial w}{\partial x}, \\ \beta_y &= \frac{\partial w}{\partial y} \end{aligned} \tag{16}$$

with x and y being Cartesian coordinates and t the time variable, and where $D = Eh^3/12(1-\nu^2)$ is the plate's bending stiffness with Young's modulus E, the plate thickness h and Poisson's ratio ν; $\nabla^4 = \partial^4/\partial x^4 + \partial^4/\partial y^4 + 2\partial^4/\partial x^2 \partial y^2$ is known as the biharmonic operator, and ρ is the mass density. $q(x, y, t)$ is the distributed vertical loading in the domain Ω.

One has to remember that this classical theory is useless for vibrations having wavelengths too short relative to the thickness of the plate. In this context, the continuous element formulation has the same limitation as finite elements. Comparisons between these two approaches should be made with a strict control of the physical validity of the solution obtained.

Under harmonic excitation, Eq. (16) can be rewritten with

$$w(x, y, t) = W(x, y)\mathrm{e}^{\mathrm{j}\omega t}, \tag{17}$$

where ω is the circular frequency. In the absence of distributed forces, $W(x, y)$ will satisfy the following equation:

$$\nabla^4 W - \frac{\rho h \omega^2}{D} W = 0. \tag{18}$$

Free boundary conditions (3) are defined on the limit of the domain $\partial\Omega$ by system (19) and force–displacement relationship (20) [18]

$$\begin{aligned} T_n + \frac{\partial M_{ns}}{\partial s} &= \mathscr{F}_z + \frac{\partial \mathscr{M}_s}{\partial s}, \\ M_n &= \mathscr{M}_n, \\ M_{ns} &= \mathscr{M}_s \end{aligned} \tag{19}$$

with

$$\begin{aligned} T_n &= -D\left(\frac{\partial^3 W}{\partial x^3} + \frac{\partial^3 W}{\partial x \partial y^2}\right) n_x - D\left(\frac{\partial^3 W}{\partial y^3} + \frac{\partial^3 W}{\partial x^2 \partial y}\right) n_y, \\ M_{ns} &= D(1-\nu)\left(\frac{\partial^2 W}{\partial x^2} - \frac{\partial^2 W}{\partial y^2}\right) n_x n_y - D(1-\nu)\frac{\partial^2 W}{\partial x \partial y}\left(n_x^2 - n_y^2\right), \\ M_n &= -D\left(\frac{\partial^2 W}{\partial x^2} + \nu\frac{\partial^2 W}{\partial y^2}\right) n_x^2 - D\left(\frac{\partial^2 W}{\partial y^2} + \nu\frac{\partial^2 W}{\partial x^2}\right) n_y^2 - 2D(1-\nu)\frac{\partial^2 W}{\partial x \partial y} n_x n_y, \end{aligned} \tag{20}$$

where $\mathscr{F}_z$, $\mathscr{M}_n$ and $\mathscr{M}_s$ are external forces applied on the limit of the domain $\partial\Omega$. $\mathbf{n}$ is the normal vector defined at each point of the boundary while n_x and n_y are its components in a Cartesian reference $(O; x, y, z)$.

3.2. General solution for rectangular plates

In the case of rectangular plates, Gorman's method of decomposition [16] allows one to obtain a general solution, similar to expression (4), for the completely free rectangular plate. Here, the only displacement component is the transverse displacement w. The rotations are obtained from derivation of w while p is equal to 1.

Once the vibration is split into four contributions, respectively, symmetric–symmetric, antisymmetric–antisymmetric, symmetric–antisymmetric and antisymmetric–symmetric, merely only a quarter segment of the completely free plate needs to be analyzed. If dimensionless plate spatial coordinates $\xi = x/a$, $\eta = y/b$ are used, a and b being the plate dimensions, the transverse displacement may be written

$$W(\xi,\eta) = W_{SS}(\xi,\eta) + W_{AA}(\xi,\eta) + W_{SA}(\xi,\eta) + W_{AS}(\xi,\eta) \tag{21}$$

S and A, respectively, designate symmetric and antisymmetric vibrations. The first letter designates the type of symmetry about y-axis, and the second about x-axis. These contributions may be expressed in terms of the total displacement $W(\xi,\eta)$ according to the following expressions (22)

$$W_{SS}(\xi,\eta) = \tfrac{1}{4}[W(\xi,\eta) + W(-\xi,-\eta) + W(-\xi,\eta) + W(\xi,-\eta)], \tag{22a}$$

$$W_{AA}(\xi,\eta) = \tfrac{1}{4}[W(\xi,\eta) + W(-\xi,-\eta) - W(-\xi,\eta) - W(\xi,-\eta)], \tag{22b}$$

$$W_{SA}(\xi,\eta) = \tfrac{1}{4}[W(\xi,\eta) - W(-\xi,-\eta) + W(-\xi,\eta) - W(\xi,-\eta)], \tag{22c}$$

$$W_{AS}(\xi,\eta) = \tfrac{1}{4}[W(\xi,\eta) - W(-\xi,-\eta) - W(-\xi,\eta) + W(\xi,-\eta)]. \tag{22d}$$

These expressions show that each contribution satisfies the equation inside domain (18) where the derivation orders with respect to spatial variables are all even. This equation could be rewritten with dimensionless variables; see Eq. (23)

$$\phi^4 \frac{\partial^4 W}{\partial \xi^4} + 2\phi^2 \frac{\partial^4 W}{\partial \xi^2 \partial \eta^2} + \frac{\partial^4 W}{\partial \eta^4} - \phi^4 \lambda^4 W = 0, \tag{23}$$

where $\phi = b/a$ is the aspect ratio of the plate and $\lambda^4 = a^4 \rho h \omega^2 / D$.

For each contribution, the general solution is obtained from the superposition of two building blocks with simple boundary conditions. These boundary conditions are simple enough to give rise to a solution expressible with Levy's series.

For example, fully symmetric solutions are obtained from the following building blocks; see Fig. 1.

The small pairs of circles indicate that the plate has zero vertical edge reaction and that the slope of the plate taken normal to the edge is equal to zero [16]. The simple boundary conditions applied on each block give rise to Levy's series type solutions (24)

$$W_{SS}(\xi,\eta) = \sum_{m=0}^{+\infty} {}^{1}_{SS}W_m(\xi) \cos m\pi\eta + \sum_{m=0}^{+\infty} {}^{2}_{SS}W_m(\eta) \cos m\pi\xi. \tag{24}$$

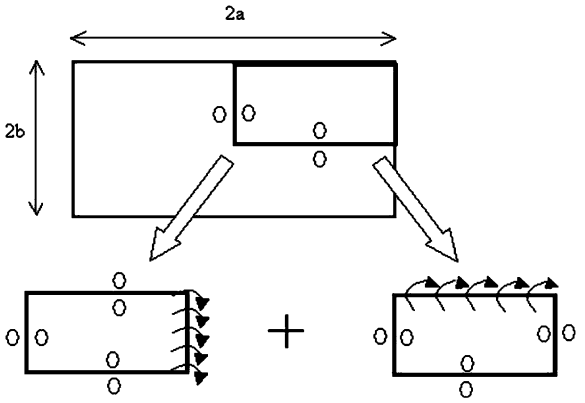

Fig. 1. Gorman's decomposition.

The even functions ${}^{1}_{SS}W_m$ and ${}^{2}_{SS}W_m$ are obtained from substituting fully symmetric solution Eq. (24) in Eq. (23). The resolution of the resulting differential equations gives

$$ {}^{1}_{SS}W_m(\xi) = A_m(e^{{}^{1}\beta_m\xi} + e^{-{}^{1}\beta_m\xi}) + B_m(e^{{}^{1}\gamma_m\xi} + e^{-{}^{1}\gamma_m\xi}) \tag{25} $$

β_m and γ_m are complex numbers given by expressions (26).

$$ {}^{1}\beta_m^2 = {}^{1}k_m^2 + \lambda^2, \tag{26a} $$

$$ {}^{1}\gamma_m^2 = {}^{1}k_m^2 - \lambda^2, \tag{26b} $$

with ${}^{1}k_m = m\pi/\phi$ and

$$ {}^{2}_{SS}W_m(\eta) = C_m(e^{{}^{2}\beta_m\eta} + e^{-{}^{2}\beta_m\eta}) + D_m(e^{{}^{2}\gamma_m\eta} + e^{-{}^{2}\gamma_m\eta}) \tag{27} $$

with

$$ {}^{2}\beta_m^2 = {}^{2}k_m^2 + \phi^2\lambda^2, \tag{28a} $$

$$ {}^{2}\gamma_m^2 = {}^{2}k_m^2 - \phi^2\lambda^2, \tag{28b} $$

where ${}^{2}k_m = \phi m\pi$.

A_m, B_m, C_m and D_m are complex integration constants.

At this stage, expression (4) is obtained for the symmetric–symmetric contribution. One could identify the required basis functions by

$$ h_{1k}(x,y) = (e^{{}^{1}\beta_k x/a} + e^{-{}^{1}\beta_k x/a})\cos\, k\pi\,\frac{y}{b}, \tag{29} $$

$$ h_{1l}(x,y) = (e^{{}^{1}\gamma_l x/a} + e^{-{}^{1}\gamma_l x/a})\cos\, l\pi\,\frac{y}{b}, \tag{30} $$

$$ h_{1m}(x,y) = (e^{{}^{2}\beta_m y/b} + e^{-{}^{2}\beta_m y/b})\cos\, m\pi\,\frac{x}{a} \tag{31} $$

and

$$h_{1n}(x,y) = (e^{{}^2\gamma_n y/b} + e^{-{}^2\gamma_n y/b}) \cos\, n\pi \frac{x}{a}. \tag{32}$$

The other contributions are obtained likewise and the corresponding basis functions h_{1n} are built. The expressions of these contributions are the following:

- antisymmetric–antisymmetric contribution:

$$W_{AA}(\xi,\eta) = \sum_{m=1}^{+\infty} {}^1_{AA}W_m(\xi) \sin \frac{(2m-1)\pi\eta}{2} + \sum_{m=1}^{+\infty} {}^2_{AA}W_m(\eta) \sin \frac{(2m-1)\pi\xi}{2} \tag{33}$$

with

$${}^1_{AA}W_m(\xi) = A_m(e^{{}^1\beta_m\xi} - e^{-{}^1\beta_m\xi}) + B_m(e^{{}^1\gamma_m\xi} - e^{-{}^1\gamma_m\xi}), \tag{34a}$$

$${}^2_{AA}W_m(\eta) = C_m(e^{{}^2\beta_m\eta} - e^{-{}^2\beta_m\eta}) + D_m(e^{{}^2\gamma_m\eta} - e^{-{}^2\gamma_m\eta}), \tag{34b}$$

${}^1\beta_m$, ${}^1\gamma_m$, ${}^2\beta_m$ and ${}^2\gamma_m$ are given by expressions (26) and (28), where ${}^1k_m = (2m-1)\pi/(2\phi)$ and ${}^2k_m = \phi(2m-1)\pi/2$.

- symmetric–antisymmetric contribution

$$W_{SA}(\xi,\eta) = \sum_{m=1}^{+\infty} {}^1_{SA}W_m(\xi) \sin \frac{(2m-1)\pi\eta}{2} + \sum_{m=0}^{+\infty} {}^2_{SA}W_m(\eta) \cos\, m\pi\xi \tag{35}$$

with

$${}^1_{SA}W_m(\xi) = A_m(e^{{}^1\beta_m\xi} + e^{-{}^1\beta_m\xi}) + B_m(e^{{}^1\gamma_m\xi} + e^{-{}^1\gamma_m\xi}), \tag{36a}$$

$${}^2_{SA}W_m(\eta) = C_m(e^{{}^2\beta_m\eta} - e^{-{}^2\beta_m\eta}) + D_m(e^{{}^2\gamma_m\eta} - e^{-{}^2\gamma_m\eta}) \tag{36b}$$

${}^1\beta_m$, ${}^1\gamma_m$, ${}^2\beta_m$ and ${}^2\gamma_m$ are given by expressions (26) and (28), where ${}^1k_m = (2m-1)\pi/(2\phi)$ and ${}^2k_m = \phi m\pi$.

- antisymmetric–symmetric contribution

$$W_{AS}(\xi,\eta) = \sum_{m=0}^{+\infty} {}^1_{AS}W_m(\xi) \cos\, m\pi\eta + \sum_{m=1}^{+\infty} {}^2_{AS}W_m(\eta) \sin \frac{(2m-1)\pi\xi}{2} \tag{37}$$

with

$${}^1_{AS}W_m(\xi) = A_m(e^{{}^1\beta_m\xi} - e^{-{}^1\beta_m\xi}) + B_m(e^{{}^1\gamma_m\xi} - e^{-{}^1\gamma_m\xi}), \tag{38a}$$

$${}^2_{AS}W_m(\eta) = C_m(e^{{}^2\beta_m\eta} + e^{-{}^2\beta_m\eta}) + D_m(e^{{}^2\gamma_m\eta} + e^{-{}^2\gamma_m\eta}) \tag{38b}$$

${}^1\beta_m$, ${}^1\gamma_m$, ${}^2\beta_m$ and ${}^2\gamma_m$ are given by expressions (26) and (28), where ${}^1k_m = m\pi/\phi$ and ${}^2k_m = \phi(2m-1)\pi/2$.

3.3. Frequency limitation

As mentioned in Section 3.1, solutions must be within the theoretical limits required by Kirchhoff's theory assumptions. Physical significance of the vibration is controlled with the ratio between the thickness of the plate and the wavelength l of the vibration. This ratio should be far less than unity. The main consequence is to restrict the frequency range as in finite element models. If we consider that the physical significance is obtained for a ratio h/l less than 0.1 and the wavelength l given by expression (39)

$$l = 2\pi \sqrt[4]{\frac{D}{\rho h \omega^2}} \tag{39}$$

one obtains

$$\omega < \frac{0.04\pi^2}{h^2} \sqrt{\frac{D}{\rho h}}. \tag{40}$$

3.4. Dynamic stiffness matrices of symmetry contributions

Matrices $\mathbf{A}(\omega)$ and $\mathbf{B}(\omega)$ used in expressions (13) and (14) are built with the help of a symbolic computation software.

The software computes the expressions of the force components owing to the force–displacement relationship (3) which are given, for the Kirchhoff theory from expressions (19) and (20). The general solution described in Section 3.2 is then truncated at rank N.

The displacement and force components are evaluated on the free edges of the quarter segment of the plate, and integration constants are factorized. This operation allows one to obtain the matrices $\partial\mathbf{H}_\omega(s)$ and $\partial\mathbf{G}_\omega(s)$ involved in expressions (7) and (8). In the case of the fully symmetric contribution, the factorizations processed are the following (41) and 42:

$$\partial\mathbf{u}(s) = \begin{pmatrix} W_{SS}(1,\eta) \\ \beta_{y_{SS}}(1,\eta) \\ W_{SS}(\xi,1) \\ \beta_{x_{SS}}(\xi,1) \end{pmatrix} = \begin{bmatrix} {}^{SS}\partial\mathbf{H}_{10}(\eta) & \dots & {}^{SS}\partial\mathbf{H}_{1N}(\eta) \\ {}^{SS}\partial\mathbf{H}_{20}(\xi) & \dots & {}^{SS}\partial\mathbf{H}_{2N}(\xi) \end{bmatrix} \begin{pmatrix} A_0 \\ B_0 \\ C_0 \\ D_0 \\ \vdots \\ A_N \\ B_N \\ C_N \\ D_N \end{pmatrix} \tag{41}$$

and

$$\partial\mathbf{f}(s) = \begin{pmatrix} F_{SS}(1,\eta) \\ M_{y_{SS}}(1,\eta) \\ F_{SS}(\xi,1) \\ M_{x_{SS}}(\xi,1) \end{pmatrix} = \begin{bmatrix} {}^{SS}\partial\mathbf{G}_{10}(\eta) & \dots & {}^{SS}\partial\mathbf{G}_{1N}(\eta) \\ {}^{SS}\partial\mathbf{G}_{20}(\xi) & \dots & {}^{SS}\partial\mathbf{G}_{2N}(\xi) \end{bmatrix} \begin{pmatrix} A_0 \\ B_0 \\ C_0 \\ D_0 \\ \vdots \\ A_N \\ B_N \\ C_N \\ D_N \end{pmatrix}. \tag{42}$$

The Hilbert basis $(e_k(s))_{k\in\mathbb{N}}$ presented in Section 2.4 is defined along each free edge of the quarter segment of the plate. This basis is

$$\left(\cos k\pi\eta, \sin\left(\frac{(2k-1)\pi\eta}{2}\right)\right)_{k\in\mathbb{N}} \quad \text{on the edge defined by } \xi = 1, \tag{43}$$

$$\left(\cos k\pi\xi, \sin\left(\frac{(2k-1)\pi\xi}{2}\right)\right)_{k\in\mathbb{N}} \quad \text{on the edge defined by } \eta = 1. \tag{44}$$

Algebraic expressions of the projections $\langle\partial H_{ij}, e_k\rangle$ and $\langle\partial G_{ij}, e_k\rangle$ involved in expressions (13) and (14) are built by the symbolic computation software and collected in the matrices $\mathbf{A}(\omega)$ and $\mathbf{B}(\omega)$. The number M of processed projections is such that resulting matrices $\mathbf{A}(\omega)$ and $\mathbf{B}(\omega)$ are square matrices, that is to say $M = N$. In the case of the fully symmetric contribution, the processed matrices are those involved in expressions (45) and (46).

$$\begin{pmatrix} {}^{\eta}_{SS}W_0 \\ {}^{\eta}_{SS}\beta_{y_0} \\ {}^{\xi}_{SS}W_0 \\ {}^{\xi}_{SS}\beta_{x_0} \\ \vdots \\ {}^{\eta}_{SS}W_N \\ {}^{\eta}_{SS}\beta_{y_N} \\ {}^{\xi}_{SS}W_N \\ {}^{\xi}_{SS}\beta_{x_N} \end{pmatrix} = \begin{pmatrix} \frac{1}{2}\int_{-1}^{1} {}^{SS}\partial\mathbf{H}_{10}(\eta)\,\mathrm{d}\eta & \dots & \frac{1}{2}\int_{-1}^{1} {}^{SS}\partial\mathbf{H}_{1N}(\eta)\,\mathrm{d}\eta \\ \frac{1}{2}\int_{-1}^{1} {}^{SS}\partial\mathbf{H}_{20}(\xi)\,\mathrm{d}\xi & \dots & \frac{1}{2}\int_{-1}^{1} {}^{SS}\partial\mathbf{H}_{2N}(\xi)\,\mathrm{d}\xi \\ \vdots & \ddots & \vdots \\ \int_{-1}^{1} {}^{SS}\partial\mathbf{H}_{10}(\eta)\cos N\pi\eta\,\mathrm{d}\eta & \dots & \int_{-1}^{1} {}^{SS}\partial\mathbf{H}_{1N}(\eta)\cos N\pi\eta\,\mathrm{d}\eta \\ \int_{-1}^{1} {}^{SS}\partial\mathbf{H}_{20}(\xi)\cos N\pi\xi\,\mathrm{d}\xi & \dots & \int_{-1}^{1} {}^{SS}\partial\mathbf{H}_{2N}(\xi)\cos N\pi\xi\,\mathrm{d}\xi \end{pmatrix} \begin{pmatrix} A_0 \\ B_0 \\ C_0 \\ D_0 \\ \vdots \\ A_N \\ B_N \\ C_N \\ D_N \end{pmatrix} \tag{45}$$

and

$$\begin{pmatrix} {}^{\eta}_{SS}F_0 \\ {}^{\eta}_{SS}M_{y_0} \\ {}^{\xi}_{SS}F_0 \\ {}^{\xi}_{SS}M_{x_0} \\ \vdots \\ {}^{\eta}_{SS}F_N \\ {}^{\eta}_{SS}M_{y_N} \\ {}^{\xi}_{SS}F_N \\ {}^{\xi}_{SS}M_{x_N} \end{pmatrix} = \begin{pmatrix} \frac{1}{2}\int_{-1}^{1} {}^{SS}\partial\mathbf{G}_{10}(\eta)\,\mathrm{d}\eta & \cdots & \frac{1}{2}\int_{-1}^{1} {}^{SS}\partial\mathbf{G}_{1N}(\eta)\,\mathrm{d}\eta \\ \frac{1}{2}\int_{-1}^{1} {}^{SS}\partial\mathbf{G}_{20}(\xi)\,\mathrm{d}\xi & \cdots & \frac{1}{2}\int_{-1}^{1} {}^{SS}\partial\mathbf{G}_{2N}(\xi)\,\mathrm{d}\xi \\ \vdots & \ddots & \vdots \\ \int_{-1}^{1} {}^{SS}\partial\mathbf{G}_{10}(\eta)\cos\,N\pi\eta\,\mathrm{d}\eta & \cdots & \int_{-1}^{1} {}^{SS}\partial\mathbf{G}_{1N}(\eta)\cos\,N\pi\eta\,\mathrm{d}\eta \\ \int_{-1}^{1} {}^{SS}\partial\mathbf{G}_{20}(\xi)\cos\,N\pi\xi\,\mathrm{d}\xi & \cdots & \int_{-1}^{1} {}^{SS}\partial\mathbf{G}_{2N}(\xi)\cos\,N\pi\xi\,\mathrm{d}\xi \end{pmatrix} \begin{pmatrix} A_0 \\ B_0 \\ C_0 \\ D_0 \\ \vdots \\ A_N \\ B_N \\ C_N \\ D_N \end{pmatrix}. \quad (46)$$

The projections of the fully symmetric transverse displacement are such that

$$W_{SS}(1,\eta) = {}^{\eta}_{SS}W_0 + \sum_{k}^{N} {}^{\eta}_{SS}W_k \cos\,k\pi\eta, \quad (47a)$$

$$W_{SS}(\xi,1) = {}^{\xi}_{SS}W_0 + \sum_{k}^{N} {}^{\xi}_{SS}W_k \cos\,k\pi\xi. \quad (47b)$$

In the case of the symmetric–symmetric contribution, the vectors composed with the projections that are the left-hand side of expressions (45) and (46) are noted $\mathbf{U}_{SS}$ and $\mathbf{F}_{SS}$. For each contribution, matrices $\mathbf{A}(\omega)$ and $\mathbf{B}(\omega)$ are built. Algebraic expressions of their components are obtained and implemented in FORTRAN instructions by the symbolic computation software. The produced instructions are used in a continuous element code library.

For each circular frequency ω, the continuous element code evaluates numerically matrices $\mathbf{A}(\omega)$ and $\mathbf{B}(\omega)$. The dynamic stiffness matrices $\mathbf{K}_{SS}(\omega)$, $\mathbf{K}_{AA}(\omega)$, $\mathbf{K}_{SA}(\omega)$ and $\mathbf{K}_{AS}(\omega)$ relative to the four contributions are obtained according to expression (15). This operation is conducted with a numerical inversion of the matrices $\mathbf{A}(\omega)$.

3.5. Dynamic stiffness matrix of the completely free rectangular plate

The dynamic stiffness matrix of the completely free plate is obtained by superpositioning of the dynamic stiffness matrices for each symmetry contribution. The principle of the superposition is described here. The displacement components along each edge are developed on the Hilbert basis. For example, the transverse displacement along the edge 1 defined by $\xi = 1$ is given by expression (48).

$$W(1,\eta) = {}^{1}W_{S_0} + \sum_{k=1}^{N} {}^{1}W_{S_k} \cos\,k\pi\eta + \sum_{k=1}^{N} {}^{1}W_{A_k} \sin\left(\frac{(2k-1)\pi\eta}{2}\right) \quad (48)$$

and along the edge 3 defined by $\xi = -1$:

$$W(-1,\eta) = {}^3W_{S_0} + \sum_{k=1}^{N} {}^3W_{S_k} \cos k\pi\eta + \sum_{k=1}^{N} {}^3W_{A_k} \sin\left(\frac{(2k-1)\pi\eta}{2}\right). \tag{49}$$

The projections ${}^1W_{S_k}$, ${}^1W_{A_k}$ and those concerning the other displacement components are collected into one vector, denoted $\mathbf{U}_e$. The components of the vector $\mathbf{U}_e$ are expressed in terms of the components of the displacement vectors of the symmetry contributions $\mathbf{U}_{SS}$, $\mathbf{U}_{AA}$, $\mathbf{U}_{SA}$ and $\mathbf{U}_{AS}$ defined above. This is done by the use of expressions (22) for each displacement component. For example, the fully symmetric transverse displacement is given by

$$W_{SS}(1,\eta) = \tfrac{1}{4}[W(1,\eta) + W(-1,-\eta) + W(-1,\eta) + W(1,-\eta)]. \tag{50}$$

Then, the use of developments Eq. (48) on each edge gives

$$W_{SS}(1,\eta) = \frac{1}{2}\left[{}^1W_{S_0} + {}^3W_{S_0} + \sum_{k=1}^{N} ({}^1W_{S_k} + {}^3W_{S_k}) \cos k\pi\eta\right] \tag{51}$$

and the identification between expressions Eqs. (47) and (51) gives

$${}^{\eta}_{SS}W_k = \tfrac{1}{2}({}^1W_{S_k} + {}^3W_{S_k}). \tag{52}$$

The identification is performed for each component of the vectors $\mathbf{U}_{SS}$, $\mathbf{U}_{AA}$, $\mathbf{U}_{SA}$ and $\mathbf{U}_{AS}$. These operations give a linear relation Eq. (53) between the vector $\mathbf{U}_e$ and the previous ones.

$$\begin{pmatrix} \mathbf{U}_{SS} \\ \mathbf{U}_{AA} \\ \mathbf{U}_{SA} \\ \mathbf{U}_{AS} \end{pmatrix} = \frac{1}{2}\,\mathbf{T}.\mathbf{U}_e. \tag{53}$$

Similar but reverse operations are conducted on the force components. For example, the vertical reaction on edge 1 is given by expression (54)

$$F(1,\eta) = F_{SS}(1,\eta) + F_{AA}(1,\eta) + F_{SA}(1,\eta) + F_{AS}(1,\eta). \tag{54}$$

The development of each contribution on the Hilbert basis is inserted in expression (54) and identification is achieved. This gives, for the vertical reaction on edge 1, with the same notations as above,

$${}^1F_{S_k} = {}^{\eta}_{SS}F_k + {}^{\eta}_{AS}F_k,$$
$${}^1F_{A_k} = {}^{\eta}_{AA}F_k + {}^{\eta}_{SA}F_k.$$

One obtains, in a matricial form,

$$\mathbf{F}_e = \mathbf{T}^{\mathrm{T}}.\begin{pmatrix} \mathbf{F}_{SS} \\ \mathbf{F}_{AA} \\ \mathbf{F}_{SA} \\ \mathbf{F}_{AS} \end{pmatrix}. \tag{55}$$

Hence, the dynamic stiffness matrix of the fully free plate, defined by expression (1), is given by expression (56).

$$\mathbf{K}(\omega) = \frac{1}{2}\,\mathbf{T}^{\mathrm{T}}.\begin{pmatrix} \mathbf{K}_{SS} & \mathbf{0} & \mathbf{0} & \mathbf{0} \\ \mathbf{0} & \mathbf{K}_{AA} & \mathbf{0} & \mathbf{0} \\ \mathbf{0} & \mathbf{0} & \mathbf{K}_{SA} & \mathbf{0} \\ \mathbf{0} & \mathbf{0} & \mathbf{0} & \mathbf{K}_{AS} \end{pmatrix}\mathbf{T}. \tag{56}$$

3.6. Numerical validation

A rectangular Kirchhoff continuous element (KCE) is implemented from the dynamic stiffness matrix Eq. (56). The results obtained by this formulation are compared with harmonic responses obtained by finite element models. A completely free rectangular plate is subjected to a unit vertical harmonic force at one of its corners. The vertical response of the structure is evaluated at the same corner; see Fig. 2.

The dimensions of the plate are $a = 0.5\,\mathrm{m}$, $b = 0.25\,\mathrm{m}$ and $h = 0.002\,\mathrm{m}$. The constitutive material is such that $E = 210{,}000 \times 10^6\,\mathrm{Pa}$, $\nu = 0.3$ and $\rho = 7800\,\mathrm{kg/m^3}$.

Now consider condition (40) as regards to this problem. One finds that the maximum circular frequency which could be considered for the Kirchhoff theory is

$$\omega_{\max} = 3.10^5\,\mathrm{rad/s} \tag{57}$$

Hence, the maximum frequency $f_{\max}$ is

$$f_{\max} = 50{,}000\,\mathrm{Hz}. \tag{58}$$

Several finite element meshings of the plate are used with three-node discrete Kirchhoff triangles (DKT) and four-node discrete Kirchhoff quadrilateral (DKQ) elements. First, the harmonic response of the plate is obtained with finite element models involving, respectively, 50×25,

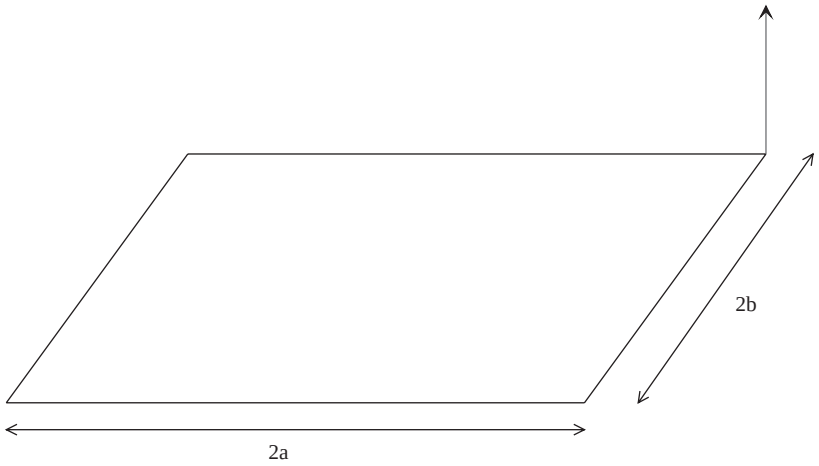

Fig. 2. Completely free rectangular plate.

100×50 and 200×100 DKT elements. The finite element solutions are obtained with the full method and are compared with an only KCE model solution. The KCE formulation involves a nine-term series. The projections of the unit force on the Hilbert basis are evaluated. One obtains

$$ {}^1F_{S_0} = \frac{1}{2b}, \quad {}^1F_{S_k} = {}^1F_{A_k} = \frac{(-1)^k}{b}. $$

The displacement of the corner is obtained from

$$ W = {}^1W_{S_0} + \sum_{k=1}^{9} {}^1W_{S_k}(-1)^k - \sum_{k=1}^{9} {}^1W_{A_k}(-1)^k. $$

The curves processed over [0−400 Hz] frequency range (which is far below the frequency limit Eq. (58)) are presented in Fig. 3. The response obtained from the 200×100 DKT model is fully converged with the KCE model results and is not represented.

A very good convergence of finite elements results toward the continuous element result can be noticed. Therefore, the precision of the continuous element formulation is obvious.

For the continuous element formulation, the number of degrees of freedom is only 136 when the numbers of degrees of freedom for finite elements formulations are, respectively, 2028, 7803 and 30,603. The bandedness of the algebraic linear system is lost but the benefit on volume of data stored in files is very significant when the structure is composed of many plates.

Afterwards, DKQ finite elements are used and the results are more precisely compared on [300−325 Hz] frequency range. This range has been chosen because an antiresonance phenomenon occurs that requires a refined finite element model. Fig. 4 shows details of the

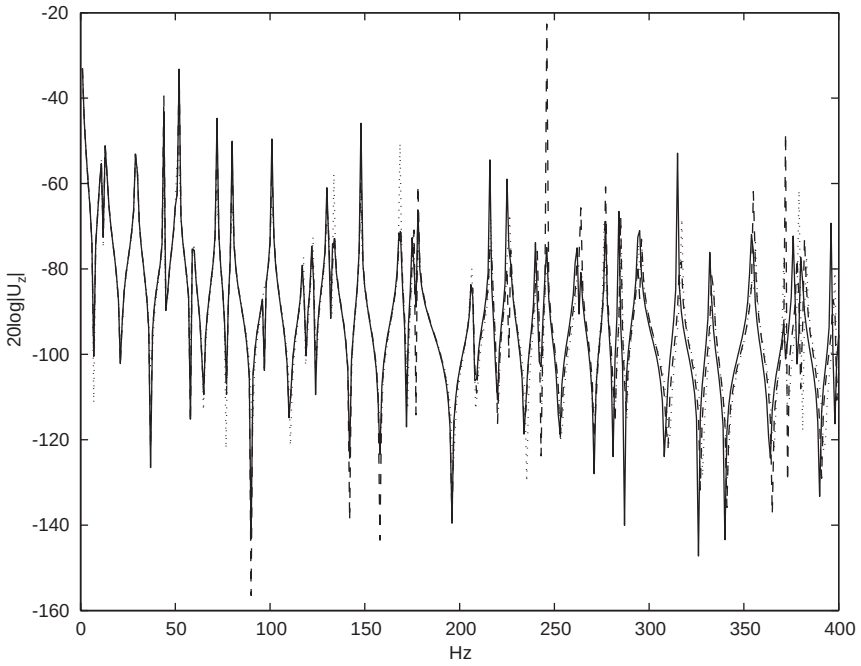

Fig. 3. Harmonic responses: —, 1 KCE; ⋯ ⋯, 50×25 DKT; — ., 100×50 DKT.

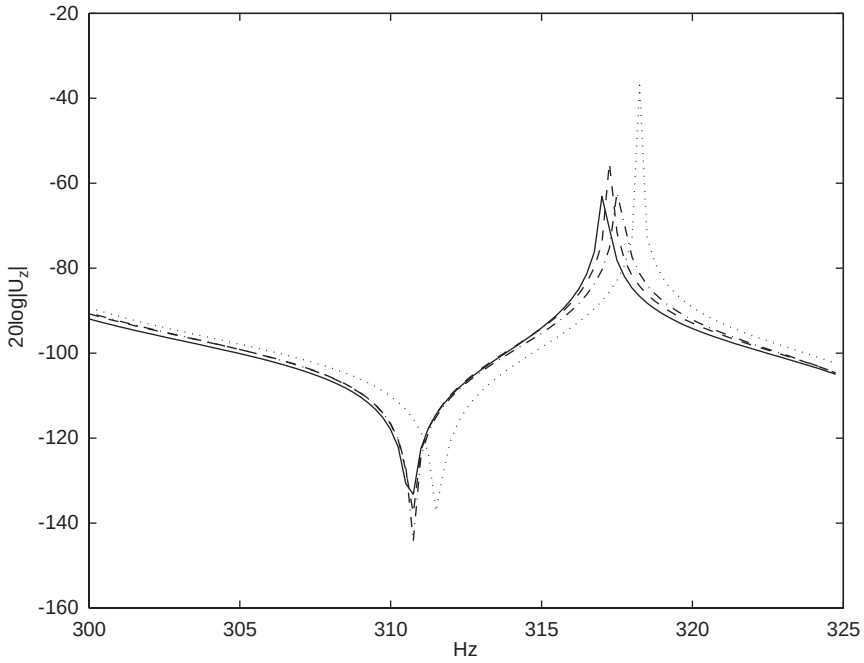

Fig. 4. Harmonic responses: —, 1 KCE; ⋯⋯, 100 × 100 DKQ; -·-·-., 150 × 150 DKQ, --- 220 × 220 DKQ.

response curves. In order to increase the precision of the finite element model, a 220 × 220 DKQ meshing is used (146, 523 dof). The finite element solutions are obtained from the modal superposition method with 250 modes taken into account.

Good convergence of finite elements results toward the continuous element result can be observed.

Higher frequency ranges have been explored in order to evaluate the numerical stability of the method. For example, the response curves on [3000−3500 Hz] are shown in Fig. 5.

The response is obtained with a 13-term EC model and a 15-term EC model. Discrepancies in the neighborhood of 3500 Hz show that at least 15 terms are required. The number of required terms increases with the frequency range. A convergence study that takes into account the number of terms is necessary for each problem. With regard to the numerical stability, no unstability has been observed when the frequency reaches its physical limit given by expression (40). The numerical stability has been estimated from the observation of the response curves. Variations of the response with the circular frequency, between resonances and anti-resonances, are quite smooth, even if the dimensions of the plate are increased. The number of required terms for such frequencies precludes a converged solution with 15 terms but the obtained response is very regular.

3.7. Post-processing

Post-processing consists of computing displacement fields inside the rectangular domain. Displacement projections $\mathbf{U}_e$ being known, expression (53) allows one to obtain displacement

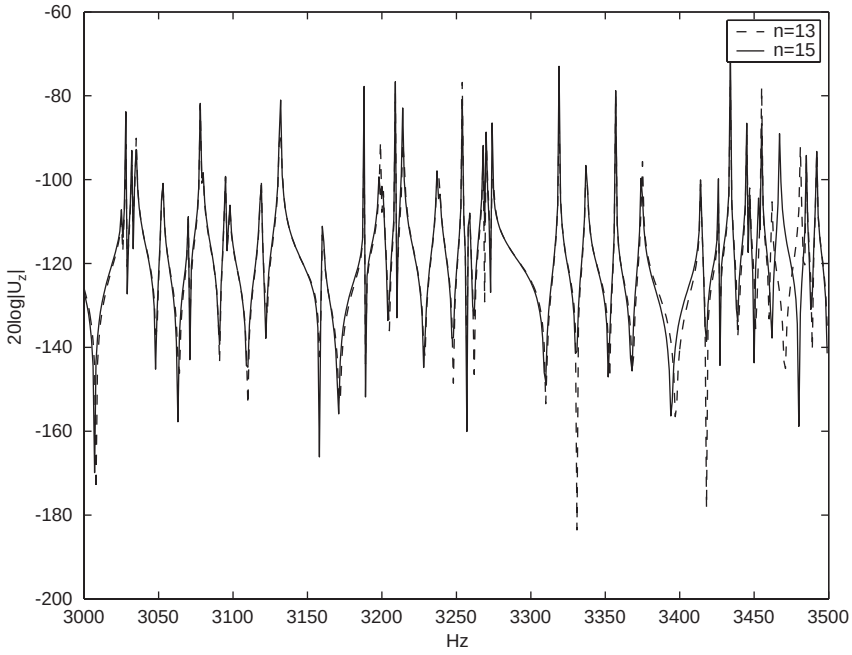

Fig. 5. Harmonic response on higher frequency range.

projections relative to each symmetry contribution. Thus, inversions of expressions similar to expression (45) give the integration constant sets $A_0, B_0, \ldots, C_N, D_N$ relative to each contribution. From these constants, it is possible to compute displacement fields according to expressions (24) and (38). Hence, the total displacement inside the domain is obtained from expression (21). For example, the transverse displacement field at 400 Hz is processed; see Fig. 6.

3.8. Damped structures

The dynamic stiffness matrix can include complex terms, so structural damping may be taken into account. The introduction of complex modulii (Young's and Coulomb's modulii as $E^* = E_0(1 + j\delta_E)$ and $G^* = G_0(1 + j\delta_G)$) is very easy. Fig. 7 shows the effect of structural damping on the harmonic response for the previous plate problem with $\delta = \delta_E = \delta_G$.

4. Conclusions

The rectangular Kirchhoff continuous element presented in this paper is particularly efficient when studying harmonic response of rectangular plates over a large frequency range. It offers a clear advantage over finite elements, particularly its high precision and low memory cost. Its performance has been evaluated on a 2 GHz Personal Computer without any optimization of algorithms. The response of the plate for 100 distinct frequencies is obtained in 10 s. This calculation speed could certainly be enhanced with judicious optimizations. The next step of the

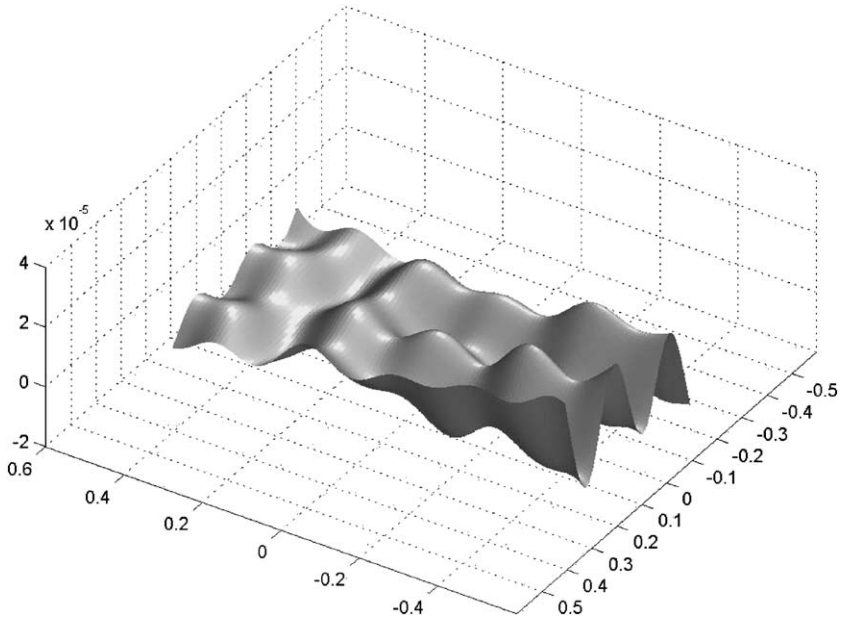

Fig. 6. Transverse displacement at 400 Hz.

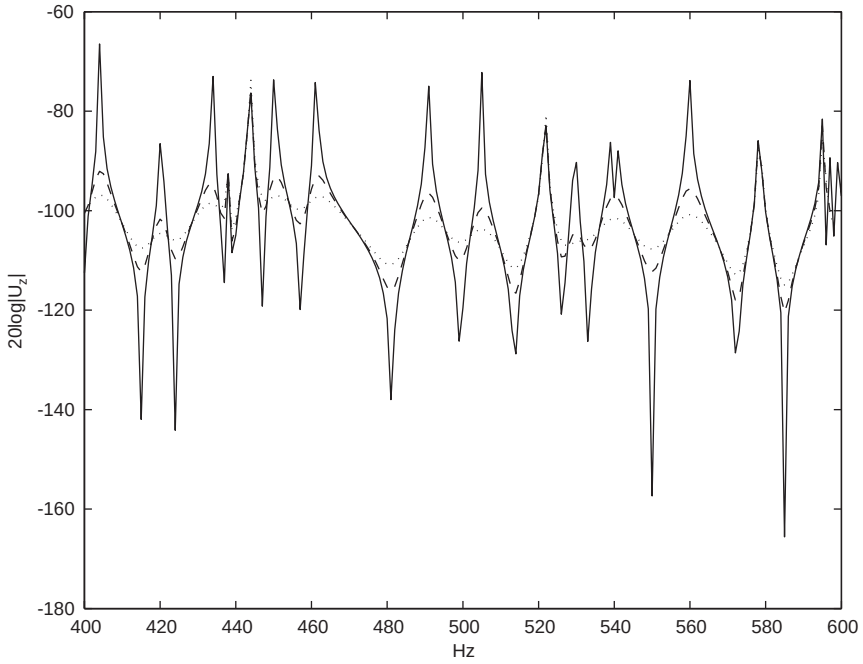

Fig. 7. Harmonic response of damped plate: —, $\delta = 0$; —, $\delta = 0.01$; ⋯, $\delta = 0.02$.

complete development of the rectangular Kirchhoff continuous element is to take in-plane vibration into account. This step is nearly completed and will be the subject of the next paper. Rectangular plates assemblies will also be considered.

References

[1] P.H. Kulla, The continuous elements method, *ESA International Conference on Spacecraft Structures and Mechanical Testing*, ESTEC, Noodwijk, The Netherlands, 1991.
[2] A.Y.T. Leung, *Dynamic Stiffness and Substructures*, Springer, London, 1993.
[3] J.B. Casimir, Eléments Continus de Type Poutre (Etude Statique et Dynamique d'Assemblages de Poutres Planes ou Gauches), Thesis in French, CNAM, 1997.
[4] J.B. Casimir, C. Duforet, T. Vinh, Dynamic behaviour of structures in large frequency range by continuous element methods, *Journal of Sound and Vibration* 267 (2003) 1085–1106.
[5] F.W. Williams, W.H. Wittrick, An automatic computational procedure for calculating natural frequencies of skeletal structures, *International Journal of Mechanical Science* 12 (1970) 781–791.
[6] J.F. Doyle, *Wave Propagation in Structures: Spectral Analysis Using Fast Discrete Fourier Transforms*, Springer, New York, 1997.
[7] U. Lee, Y.T. Leung, The spectral element method in structural dynamics, *The Shock and Vibration Digest* 32 (2000) 451–465.
[8] C. Duforêt, Dynamic study of an assembling of rods in medium and higher frequency ranges—computer code ETAPE, *Third Colloquium on New Trends in Structure Calculations—Bastia, Corsica—Proceedings*, 1985, pp. 229–246 (in French).
[9] M.S. Anderson, F.W. Williams, J.R. Banerjee, B.J. Durling, C.L. Herstorm, D. Kennedy, D.B. Warnaar, User Manual for BUNVIS-RG: an exact buckling and vibration program for lattice structures, with repetitive geometry and substructuring options, NASA Technical Memorandum 87669, 1986.
[10] F.W. Williams, D. Kennedy, R. Butler, M.S. Anderson, VICONOPT: program for exact vibration and buckling analysis or design of prismatic plate assemblies, *AIAA Journal* 29 (1991) 1927–1928.
[11] P.H. Kulla, Continuous elements, some practical examples, *ESTEC Workshop Proceedings: Modal Representation of Flexible Structures by Continuum Methods*, 1989.
[12] S. Kevorkian, M. Pascal, An accurate method for free vibration analysis of structures with application to plates, *Journal of Sound and Vibration* 246 (5) (2001) 795–814.
[13] H. Le Sourne, Développement d'Éléments Continus de Coques Axisymétriques et de Coudes, Thesis in French, Université de Nantes, 1998.
[14] R.D. Mindlin, Influence of rotary inertia and shear in flexural motion of isotropic elastic plates, *Journal of Applied Mechanics* 18 (1951) 31–38.
[15] A.W. Leissa, *Vibration of Plates*, NASA SP160 Publications, 1968.
[16] D.J. Gorman, *Free Vibration Analysis of Rectangular Plates*, Elsevier, Amsterdam, 1982.
[17] P. Hagedorn, K. Kelkel, J. Wallascheck, *Vibration and Impedance of Rectangular Plates with Free Boundaries*, Lecture Notes in Engineering, Springer, Berlin, 1986.
[18] J.L. Batoz, G. Dhatt, *Modélisation des Structures par Éléments Finis*, Hermes, Paris, 1990.